Eur. Phys. J. B **16**, 705–718 (2000)

THE EUROPEAN PHYSICAL JOURNAL B

EDP Sciences

Understanding of surface states in a correlated electron system

W. Müller[a], R. Schiller, and W. Nolting

Institut für Physik, Humboldt-Universität zu Berlin, Invalidenstraße 110, 10115 Berlin, Germany

Received 8 March 2000

Abstract. The aim of this work is to find a simple analytic model to explain some principal aspects of the behavior of surface states in correlated electron systems. We start from the analytic expression for the Green function of the semi-infinite tight binding linear chain. This Green function in case of modification of the center of gravity of the first atom and the change in coupling between the first and the second atom is evaluated as an exact analytic expression. Conditions for the existence and classification of surface states are given. The spectral weight of surface states and the local density of states are evaluated. The method is applied to a s.c. (100) surface of a local moment crystal. Conditions for the existence of surface states are derived and their locations in the Brillouin zone are predicted. It is shown that it is possible to include correlation effects within the framework of the discussed model. The comparison with former numerical results is performed.

PACS. 75.70.-i Magnetic films and multilayers – 73.20.At Surface states, band structure, electron density of states – 75.50.Pp Magnetic semiconductors

1 Introduction

Surfaces are the boundaries between different phases of matter and are the reason for many interesting phenomena. We are in particular interested in the influence of the surface on the electronic structure.

The behavior of the surface states in correlated local moment films [1,2] was the motivation for this article which was announced in [1] as to be published. This work provides the key to understand the general features in the spectra of the surfaces of correlated electron systems. Some known aspects which are important for the understanding are used to develop an analytical description for surface states showing the conditions for existence, position in energy as well as spectral weight of a surface state on a given point in the two dimensional Brillouin zone. That shell help to interpret the results of more complex calculations [1,2].

In 1932 Tamm indicates for the first time the existence of specific electron states, later called "*Tamm states*", localized near the crystal surface. His paper "On the possible bound states of electrons on a crystal surface" [3] is the starting point for the *Surface Science*. In the following years the theoretical research activity was intense (Fowler [4], Sokolov [5], Maue [6] and Goodwin [7]). In 1939 Shockley [8] explained how surface states originate from the atomic levels, as the crystal is built up by lowering the lattice constant from infinity to a finite value. After Shockley's publication, the general trend was in literature to distinguish between *Shockley* and *Tamm surface states*. Shockley states occur within hybridizational band gaps far from the band edges and require a multi band model. Tamm states were considered as completely originating from the change in the potential in the outermost crystal cell and they are located near by the band edges. For completeness the *image states* should mentioned which are located mainly outside the crystal. A good introduction to the theory of surface states is given in the review article by Davison and Levine [9] and in the later book by Davison and Stręślicka [10].

In the next section the Hamiltonian for the semi-infinite crystal is introduced, in Section 3 the model of the semi-infinite chain is solved using a Green function approach. The modification of the center of gravity of the first atom and the change in coupling between the first and the second atom is taken into account. We get exact results for all elements of the Green function, the position in energy and spectral weight of surface states for each site.

The results are then applied to a s.c. (100) surface of a local moment crystal in Section 4. We map for each wave vector on the chain model. The spectral density is discussed for the free surface.

Finally, in Section 5 the interplay of surface states and the spin exchange correlation in a local moment film is shown. We compare the results of our analytic model with the numerical results [1].

[a] e-mail: wolf.mueller@physik.hu-berlin.de

2 Hamiltonian of the surface of semi-infinite crystals

The Hamiltonian of the semi-infinite extended crystal can be expressed by

$$\mathbf{H} = \sum_{ij} \sum_{\alpha,\beta=1}^{\infty} h_{ij}^{\alpha\beta}, \tag{1}$$

where $\alpha, \beta = 1, 2, \ldots$ are the layer indices and i, j number the sites within the layers. Because of the two dimensional translational invariance we perform the Fourier transformation,

$$\mathbf{H} = \sum_{\mathbf{k}} \sum_{\alpha,\beta=1}^{\infty} h_{\alpha\beta}(\mathbf{k}), \tag{2}$$

where $\mathbf{k}$ is the 2-dimensional wave vector and

$$h_{\alpha\beta}(\mathbf{k}) = \frac{1}{N} \sum_{ij} \mathrm{e}^{\mathrm{i}\mathbf{k}(\mathbf{R}_i - \mathbf{R}_j)} h_{ij}^{\alpha\beta}, \tag{3}$$

$\mathbf{R}_i$ and $\mathbf{R}_j$ are 2-dimensional lattice vectors. For simplicity, we restrict ourselves to the tight binding approximation and to the surfaces for which the resulting 2-dimensional wave vector dependent Hamiltonian $\mathbf{h}(\mathbf{k})$ becomes tridiagonal (surfaces for which the next neighbors are in the same or in the next layer, *e.g.* sc(100), sc(110), sc(111), bcc(100), bcc(100), bcc(110), fcc(100), fcc(111)). In case of uniform hopping between the next neighbors the dispersions parallel and perpendicular to the surface are given by

$$\gamma_{||}(\mathbf{k}) = \sum_{j}^{\mathbf{R}_{i\alpha},\mathbf{R}_{j\beta}\ \text{n.n.};\ \alpha=\beta} \mathrm{e}^{-\mathrm{i}\mathbf{k}(\mathbf{R}_i - \mathbf{R}_j)}, \tag{4}$$

$$\gamma_{\perp}^{\pm}(\mathbf{k}) = \sum_{j}^{\mathbf{R}_{i\alpha},\mathbf{R}_{j\beta}\ \text{n.n.};\ \alpha=\beta\pm1} \mathrm{e}^{\pm\mathrm{i}\mathbf{k}(\mathbf{R}_i - \mathbf{R}_j)}. \tag{5}$$

For all cubic crystals $\gamma_{||}$ is real but $\gamma_{\perp}^{\pm}$ can be complex. In case of sc(100), sc(110), bcc(100), bcc(100), bcc(110), and fcc(100) also the perpendicular dispersion is real ($\gamma_{\perp} = \gamma_{\perp}^{+} = \gamma_{\perp}^{-}$). The perpendicular dispersion considering the next neighbors in the layer below and above are given by $\gamma_{\perp}^{-}$ and by $\gamma_{\perp}^{+}$ respectively. $\gamma_{\perp}^{-}$ and $\gamma_{\perp}^{+}$ are conjugate complex to each other. The expressions for the various geometries can be found in Appendix A. Now the Hamiltonian can be interpreted as an ensemble of semi infinite linear chains for each $\mathbf{k}$-point

$$\mathbf{H} = \sum_{\mathbf{k}} \mathbf{h}(\mathbf{k}). \tag{6}$$

In general the $\mathbf{k}$-dependent Hamiltonian is hermitian but not symmetric. However, if we are interested in the diagonal elements of the Green function only, the hermitian Hamiltonian and the symmetric Hamiltonian formed by substituting the off-diagonal elements by its absolute value yield the same result [11]. In that sense it is no limitation that the approach presented in the next Section 3 uses the symmetric input equations (7, 16).

3 Green function of semi-infinite linear atomic chain

3.1 Ideal linear chain

The Hamilton operator of an atomic chain in tight-binding approximation is given by

$$\mathbf{h_0} = \begin{pmatrix} \alpha & -\gamma & 0 & \cdots \\ -\gamma & \alpha & -\gamma & \ddots \\ 0 & -\gamma & \alpha & \ddots \\ \vdots & \ddots & \ddots & \ddots \end{pmatrix}, \tag{7}$$

where α is the center of gravity and 2γ is the total bandwidth of the s-band of the atoms of the chain. Furthermore the Green function of the system is defined by

$$(\mathbf{h_0} - E\mathbf{I})\, \mathbf{G}^0(E) = -\hbar\, \mathbf{I}. \tag{8}$$

We measure the energy E in units of bandwidth *i.e.* we introduce the "reduced" energy

$$t = \frac{E - \alpha}{2\gamma}\,. \tag{9}$$

Using the substitution for the reduced energy

$$-t = \cos\theta, \tag{10}$$

where $\theta \in \mathbb{C}$, the elements of the Green function matrix of ideal atomic tight binding chain can be given in an analytical form as presented in Appendix B (Eqs. (B.1-B.4))

$$\left(\mathbf{G^0}\right)_{kl} = g_{kl}^0 = -\frac{\hbar}{\gamma}\, \frac{\mathrm{e}^{\mathrm{i}(k+l)\theta} - \mathrm{e}^{\mathrm{i}|k-l|\theta}}{2\mathrm{i}\sin\theta} \tag{11}$$

where $\theta = \arccos(-t)$. The following identities hold:

$$g_{kl}^0 = g_{lk}^0, \tag{12}$$

$$g_{21}^{0\ 2} - g_{11}^0\, g_{22}^0 = g_{21}^0 \hbar/\gamma. \tag{13}$$

3.2 Perturbation and defect matrix method

Now we would like to include into our model chain a perturbation induced by the cut off of the chain which is expressed by a displacement of the center of gravity of the band at the first atom $\alpha \to \alpha'$ and by a change of coupling between first and second atom $\gamma \to \gamma'$. The Hamiltonian $\mathbf{h}$ differs in the 3 elements $(\mathbf{h})_{11} = \alpha'$ and $(\mathbf{h})_{12} = (\mathbf{h})_{21} = \gamma'$ from $\mathbf{h_0}$ only. The Green function for this generalized problem is defined by

$$(\mathbf{h} - E\,\mathbf{I})\, \mathbf{G}(E) = -\hbar\, \mathbf{I}. \tag{14}$$

In order to find the solution we use the method of defect matrix, proposed and used by Maradudin [12] and

Pollmann [13], *i.e.* we split $\mathbf{h}$ into one matrix representing the ideal semi infinite chain and the rest $\delta\mathbf{h}$, which is called the "defect matrix":

$$\mathbf{h} = \mathbf{h_0} + \boldsymbol{\delta}\mathbf{h}. \tag{15}$$

The defect matrix is rather trivial and except the three elements

$$h_1 = (\delta\mathbf{h})_{11} = \alpha' - \alpha,\ \ h_2 = (\delta\mathbf{h})_{12} = (\boldsymbol{\delta}\mathbf{h})_{21} = -\gamma' + \gamma \tag{16}$$

all elements are equal zero. We combine equations (8, 14) to the *Dyson's equation* [14] and we obtain

$$\mathbf{G}(E) = \left[\mathbf{I} - \frac{1}{\hbar}\,\mathbf{G}^0(E)\boldsymbol{\delta}\mathbf{h}\right]^{-1}\mathbf{G}^0(E). \tag{17}$$

The matrix inversion of

$$\mathbf{A} = \mathbf{I} - \frac{1}{\hbar}\,\mathbf{G^0}\,\boldsymbol{\delta}\mathbf{h} \tag{18}$$

is simple and straight-forwardly done in Appendix C. The multiplication of $\mathbf{A}^{-1}$ (Eq. (C.2)) with the Green function of the ideal problem yields *all* elements of the Green function of the semi-infinite perturbed linear chain

$$\begin{aligned} G_{1j} &= \frac{1}{\lambda}\left(a_{22}\,g^0_{1j} - a_{12}\,g^0_{2j}\right),\\ G_{2j} &= \frac{1}{\lambda}\left(-a_{21}\,g^0_{1j} + a_{11}\,g^0_{2j}\right),\\ G_{ij} &= \frac{1}{\lambda}\left(\begin{vmatrix} a_{21} & a_{i1}\\ a_{22} & a_{i2}\end{vmatrix} g^0_{1j} - \begin{vmatrix} a_{11} & a_{i1}\\ a_{12} & a_{i2}\end{vmatrix} g^0_{2j}\right) + g^0_{ij} \text{ for } i \geq 3, \end{aligned} \tag{19}$$

where

$$\begin{aligned} a_{i1} &= \delta_{i1} - (g^0_{i1}h_1 + g^0_{i2}h_2)/\hbar,\\ a_{i2} &= \delta_{i2} - g^0_{i1}h_2/\hbar \end{aligned} \tag{20}$$

and

$$\lambda = \begin{vmatrix} a_{11} & a_{21}\\ a_{12} & a_{22}\end{vmatrix} = \det\mathbf{A}. \tag{21}$$

Our result is the same as found in [15] (Eq. (27)) and [16] (Eq. (2.16)) if we restrict ourselves to the diagonal elements of the Greens function and the simpler case of only changed center of gravity of the first atom. The expressions of the Green function for the first and second atom of the chain are especially simple

$$G_{11} = \frac{1}{\lambda}\,g^0_{11}, \tag{22}$$

$$G_{22} = \frac{1}{\lambda}\left(g^0_{22} + \frac{h_1}{\gamma}g^0_{21}\right). \tag{23}$$

This can be obtained by equations (12, 13).

3.3 Existence of surface states

In this subsection we are interested in the surface states which may occur dependent on the shift of center of gravity of the band of the first atom and on the change of the coupling between first and second atom (Tamm states [3]). The diagonal elements of the Green function can be written as

$$G_{nn}(t) = \frac{1}{\lambda}R_n(t) + S_n(t), \tag{24}$$

where $R_n(t)$ and $S_n(t)$ are functions built up from g^0_{ij} which contain only poles $t_n \in [-1, 1]$ included in the original Green function of ideal semi-infinite linear chain. $R_n(t)$ is given by

$$\begin{aligned} R_1 &= g^0_{11},\\ R_2 &= g^0_{22} + \frac{h_1}{\gamma}g^0_{21},\\ R_{n\geq 3} &= \begin{vmatrix} a_{21} & a_{n1}\\ a_{22} & a_{n2}\end{vmatrix} g^0_{1j} - \begin{vmatrix} a_{11} & a_{n1}\\ a_{12} & a_{n2}\end{vmatrix} g^0_{2j}. \end{aligned} \tag{25}$$

The exact shape of $S_n(t)$ which can be found by subtraction of equation (25) from equation (19) is of no interest. We are now looking for poles which have an reduced energy outside the bulk band $|t_i| > 1$. The only reason for surface states are poles introduced by the roots of the denominator (21)

$$\lambda(t) = \hbar^2 - \hbar g^0_{11}h_1 - 2\hbar g^0_{21}h_2 + \left({g^0_{21}}^2 - g^0_{11}g^0_{22}\right)h_2^2 = 0. \tag{26}$$

If we use the identities (13, 12) only the elements g^0_{11} and g^0_{21} of the Green function $\mathbf{G^0}$ occur in equation (26). Due to equation (11) they can be expressed by

$$z = \mathrm{e}^{-\mathrm{i}\theta} \tag{27}$$

as

$$g^0_{11} = -\frac{\hbar}{\gamma}\,z^{-1} \qquad \text{and} \qquad g^0_{21} = -\frac{\hbar}{\gamma}\,z^{-2}\,. \tag{28}$$

The connection between the reduced energy t and the variable z *via* equations (10, 27) can be written as

$$-t = \cos\theta = \tfrac{1}{2}\left(z^{-1} + z\right). \tag{29}$$

Furthermore it is convenient to give the elements of the defect matrix in units of the bandwidth

$$\tilde{h}_1 = h_1/2\gamma \quad \text{and} \quad \tilde{h}_2 = h_2/\gamma. \tag{30}$$

Now equation (26) yields

$$\lambda(z) = \frac{\hbar^2}{z^2}\left(z^2 + 2z\tilde{h}_1 + 2\tilde{h}_2 - \tilde{h}_2^2\right) = 0. \tag{31}$$

Two properties of a physical solution of equation (31) $z = \exp(-\mathrm{i}\theta)$ are demanded. First the reduced energy

Table 1. Classification of solutions for z.

type of solution	root	reduced energy
bulk states	$\|z\| = 1$	$-1 \leq t \leq 1$
lower surface states	$z > 1$	$t < -1$
upper surface states	$z < -1$	$t > 1$
asymptotic divergent	$-1 < z < 1$	$\|t\| > 1$

$t = -\cos\theta$ has to be real, second the solution has to possess the correct asymptotic behavior. In a sufficiently large distance from the surface ($n, m \gg 1$) the Green functions of the ideal and the perturbed chain are equal. If we fix m and if we assume $n \geq m$ we find because of equation (11) that

$$G_{nm} \sim \mathrm{e}^{\mathrm{i}n\theta} \qquad (n > m \gg 1). \tag{32}$$

Bulk states are obviously obtained if $\theta = ka \in \mathbb{R}$, where k is the wave vector and a is the lattice constant. The Green function is

$$|G_{nm}| \sim |\mathrm{e}^{\mathrm{i}nka}| = 1 \tag{33}$$

uniformly distributed because of equation (32). The solution for an electron is a plane wave.

Surface states satisfy the first condition using $\theta = \sigma + \mathrm{i}\tau \in \mathbb{C}$, where $\sigma, \tau \in \mathbb{R}$. A real reduced energy

$$t = -\cos\theta = -\cos\sigma\cosh\tau + \mathrm{i}\sin\sigma\sinh\tau \tag{34}$$

can be obtained either with $\sigma = 0$ or $\sigma = \pi$. The absolute value of the Green function sufficiently far from the surface is given by

$$|G_{nm}| \sim \mathrm{e}^{-n\tau}. \tag{35}$$

To assure the correct asymptotic behavior we have to choose $\tau > 0$.

The solution $\theta = \mathrm{i}\tau$ results in a surface state with an reduced energy $t = -\cosh\tau < -1$ below the bulk band and there is no phase shift between neighboring atoms. We call it *lower surface state* in the following. It exponentially goes to zero from the surface into the bulk.

The other solution $\theta = \pi + \mathrm{i}\tau$ we call an *upper surface state* because there is an phase shift π between neighboring atoms. The reduced energy of this state $t = \cosh\tau > 1$ is located above the bulk band. It also goes to zero from the surface into the bulk.

The results are summarized in the Table 1. The surface states we are interested in are qualified by $|z| > 1$ and $z \in \mathbb{R}$. In case of a vanishing defect matrix ($\tilde{h}_1 = \tilde{h}_2 = 0$) we have no solution for surface states. If $\tilde{h}_2 = 0$ and $\tilde{h}_1 \neq 0$, one surface state is possible

$$z_1 = -2\tilde{h}_1, \tag{36}$$

otherwise up to two surface states can exist

$$z_{1,2} = -\tilde{h}_1 \pm \sqrt{\tilde{h}_1^2 + \tilde{h}_2^2 - 2\tilde{h}_2}. \tag{37}$$

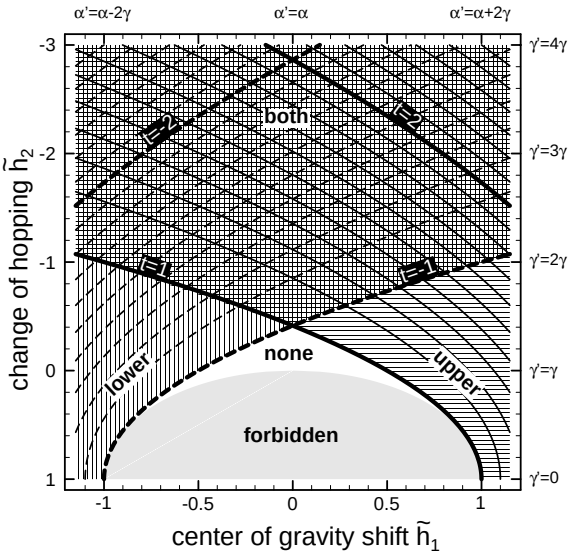

Fig. 1. Phase diagram of surface states for shifts of center of gravity $\tilde{h}_1 \in (-1.1, 1.1)$ and change of hopping between first and second atom $\tilde{h}_2 \in (-3, 1)$. The solid lines show the reduced energies of surface states above the bulk band. The dashed lines show the reduced energies below the bulk band. There are four regions: no surface states (either no real reduced energies or wrong asymptotic behavior), lower surface state, upper surface state, and upper and lower surface state.

Because z has to be real there is a forbidden parameter region $\tilde{h}_1 + \tilde{h}_2^2 - 2\tilde{h}_2 < 0$ which is plotted gray in Figure 1. Consequently surface states can exist outside only. On the basis of the criteria in Table 1 and because of the solutions (36, 37) we can construct the phase diagram with respect to surface states dependent on the parameters $\tilde{h}_1$ (shift of center of gravity at first atom) and $\tilde{h}_2$ (change of hopping between first and second atom) shown in Figure 1. No surface states occur for small center of gravity shifts and small modification of hopping between first and second atom. The area of no surface states is composed of the grey "forbidden" region where no solutions exist and the white plotted region where the existent solutions have the wrong asymptotic behavior. This area ranges from $\tilde{h}_1 = \pm 1$, $\tilde{h}_2 = 1$ over $\tilde{h}_1 = \pm\frac{1}{2}$, $\tilde{h}_2 = 0$ to $\tilde{h}_1 = 0$, $\tilde{h}_2 = 1 - \sqrt{2}$. This region is limited by the solid line $t = 1$ joining the parameters for which upper surface states split from bulk band at higher energies and the dashed line $t = -1$ showing those for lower ones which split off at lower energies. For center of gravity shifts larger than half bandwidth ($\tilde{h}_1 > \frac{1}{2}$) the upper surface state appears. For shifts in the opposite direction ($\tilde{h}_1 < -\frac{1}{2}$) the lower surface state occurs. If the modification of hopping between first and second atom becomes large enough $\tilde{h}_2 < 1 - \sqrt{2}$ both lower and upper surface state can exist. For $\tilde{h}_2 = 1$ which means a complete decoupling of the first atom from the chain ($\gamma' \equiv 0$: Eqs. (16, 30)) we obtain one surface state only if the center of gravity shift is larger than the total bandwidth($|\tilde{h}_1| > 1$).

The reduced energies t belonging to the surface states are given by the solid lines and dashed lines, respectively. The larger the modification of hopping $\tilde{h}_2$ the larger the energy distance from bulk band.

3.4 Spectral weight of surface states

We are interested in the spectral weight of surface states *i.e.* $|z| > 1$. For this situation $R_n(t)$ and $S_n(t)$ introduced in equation (24) represent only real continuous functions without poles. We assume for the solutions of equation (31) without restrictions

$$z_1 > 0 > z_2 \;\Leftrightarrow\; t_1 < 0 < t_2. \tag{38}$$

The spectral weight of a surface state at the energy E_i is denoted by $\alpha_i^{(n)}$ $(i = 1, 2)$ where (n) indicates the chain atom. The weights are found by:

$$\begin{aligned}\alpha_i^{(n)} &= \lim_{E\to E_i} (E - E_i)\, G_{nn}(E) \\ &\overset{(9)}{=} 2\gamma \lim_{t\to t_i} \left\{ (t - t_i) \left(\frac{1}{\lambda} \cdot R_n(t) + S_n(t) \right) \right\} \\ &= 2\gamma\, R_n(t_i) \cdot \lim_{t\to t_i} \frac{t - t_i}{\lambda(t)}. \end{aligned} \tag{39}$$

We look for the ratio of spectral weights what is given by the ratio of the functions R_m and R_n

$$\frac{\alpha_i^{(m)}}{\alpha_i^{(n)}} = \frac{R_m(t_i)}{R_n(t_i)}\,. \tag{40}$$

Thus all spectral weights can be written

$$\alpha_i^{(n)} = \frac{\alpha_i^{(1)}}{g_{11}^0(t_i)}\, R_n(t_i), \tag{41}$$

where $R_n(t_i)$ is known from equation (25).

We have now only to determine the spectral weights of surface states for the first atom. This is done in Appendix D inserting equations (28, 25) into equation (41)

$$\alpha_i^{(1)} = -2 \lim_{t\to t_i} \frac{t - t_i}{z(t)\, \lambda(z(t))}\,. \tag{42}$$

The resulting spectral weights of surface states at the first atom given in equations (D.4-D.11) are shown in Figure 2 for the upper case. The spectral weight is proportional to the height as well as to the gray level of the plotted point. White means no surface states are present. The regions where upper surface states exist can be easily recognized. The surface states at equal positions in energy are joined by the black solid lines. We observe the larger the distance in energy from the bulk band the larger the spectral weight of a surface state becomes. If the energy of a surface state is very close to the bulk band ($|t_i| \gtrapprox 1$) the spectral weight of it tends to zero. In the limit of $\tilde{h}_1 \to \pm\infty$ the full spectral weight is very soon represented by the upper peak and lower peak, respectively. If we sufficiently strong increase the coupling between the first and second atom $\tilde{h_2} \to -\infty$ and fix $\tilde{h_1} = 0$ the spectral weight is symmetrically distributed between the peak below and above the bulk band and we obtain $\frac{1}{2}$ as limit value. In the limit of complete decoupling of the first from the second atom ($\tilde{h}_2 \to 1$) we have only an upper surface state if the center of gravity shift is larger than the total bandwidth ($\tilde{h}_1 > 1$). Its reduced energy is given by its shift $\tilde{h}_1$ and it has the full spectral weight 1. The spectral weights of lower surface states are completely analogous. The phase diagram presented in Figure 1 can be understood as the projection of the stack of the two 3-dimensional graphics of the upper surface states and of the lower one (obtained by mirroring on the $\tilde{h}_1 \equiv 0$ plane).

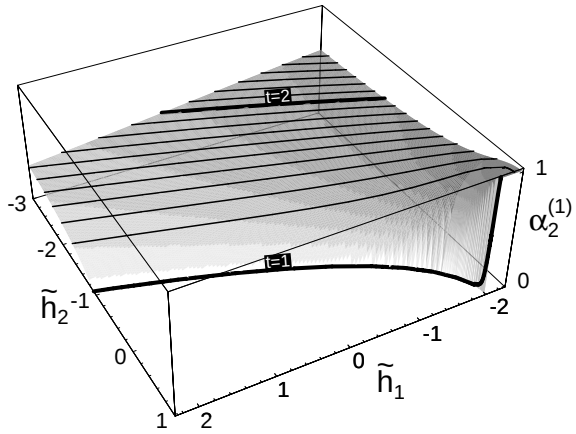

Fig. 2. Spectral weight of the upper surface state dependent of the center of gravity shift of first atom $\tilde{h}_1$ and the change in coupling between the first and second atom $\tilde{h}_2$ represented by the height as well as by the gray level of the current point. The black lines give the reduced energy t of the surface peak.

3.5 Local density of states

The physical behavior is best monitored by the *local density of states* (LDOS) for a given atom n. The LDOS is derived from the imaginary part of the diagonal Green functions (Eqs. (11, 19))

$$\rho_n^{(0)} = -\frac{1}{\pi} \Im G_{nn}^{(0)}. \tag{43}$$

In contrast to the infinitely extended linear chain the LDOS ρ_n^0 depends on the site n in the chain. For surface near atoms this dependence presented in Figure 3 is drastic. The LDOS at the first atom ($n = 1$) is a semi-elliptic one and has no zeros. By incrementing the distance from surface by one atom one zero or one oscillation is added. For large $n \to \infty$ the shape of LDOS approaches the one dimensional tight-binding density of states.

Now we consider the modification of the LDOS of the first site of the chain $n = 1$ in the case of a change of center of gravity of the first atom expressed by $\tilde{h}_1$ and in the case of change of coupling between first and second

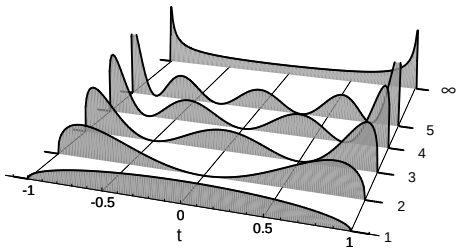

Fig. 3. LDOS ρ_n^0 from the 1st up to 5th atom and the inner atom (∞) of the ideal semi-infinite linear chain as function of the reduced energy t.

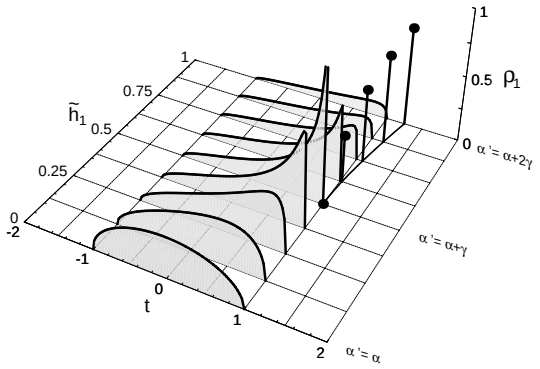

Fig. 4. The local density of states of the first atom as a function of the reduced energy and for various shifts of the center of gravity $\tilde{h}_1$. The coupling between all atoms remains constant.

atom of the chain $\tilde{h}_2$ (Eqs. (16, 30)). The general LDOS is given by the imaginary part of Green function (19)

$$\rho_n = -\frac{1}{\pi} \Im\, G_{nn}. \tag{44}$$

If we shift only the center of gravity of the first atom towards higher reduced energies the shape of LDOS is changed from the semi elliptic in an asymmetric one (see Fig. 4). For strong enough shifts $\tilde{h}_1 > \frac{1}{2}$ (half bandwidth) a surface state splits off which is plotted as a thick point. The height of this point represents the spectral weight of the surface peak starting from zero at $\tilde{h}_1 = \frac{1}{2}$ and approaching 1 for huge center of gravity shifts. The spectral weight in the range of bulk energies $t \in (-1, 1)$ shows the opposite behavior.

Figure 5 offers the LDOS of the first atom in the case of a coupling change between the first and the second atom. If we reduce the coupling ($\tilde{h}_2 > 0$) the LDOS narrows and for $\tilde{h}_2 = 1$ which means a complete decoupling of the first atom from the rest of the chain it becomes the atomic level. If we increase the coupling between these layers ($\tilde{h}_2 < 0$) spectral weight is moved symmetrically from the center to the edges. The surface states occurring for $\tilde{h}_2 < 1 - \sqrt{2}$ become more and more pronounced and the spectral weight within the bulk band energy range drops rapidly. For strong coupling of the first and second atom the complete spectral weight is evenly distributed between the both surface states.

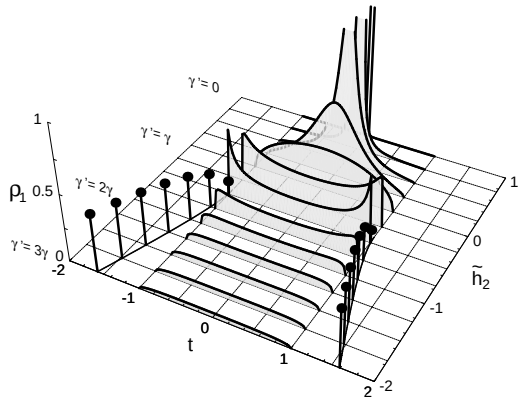

Fig. 5. The local density of states of the first atom dependent on the energy and the coupling between first and second atom. The center of gravity of all atoms is the same.

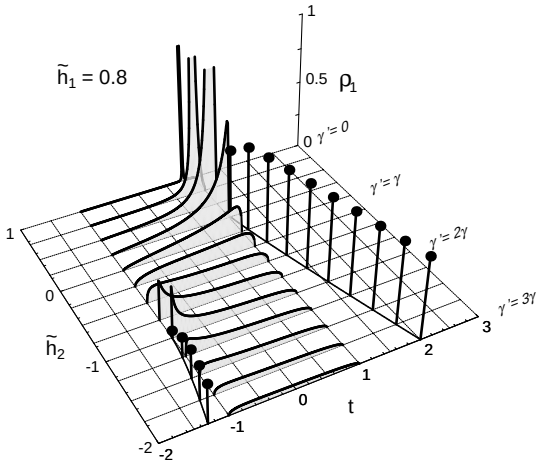

Fig. 6. LDOS of the first atom dependent on the reduced energy and the coupling between the first and second atom for a fixed shift of the center of gravity of 0.8 total bandwidths.

If we additionally add a center of gravity shift smaller than the total bandwidth $\tilde{h}_1 = 0.8 < 1$ we obtain the picture of the LDOS as function of coupling change between first and second atom presented in Figure 6. The symmetry is of course destroyed as a consequence of the shift of the center of gravity. If a surface state is very close to the bulk band edge the spectral weight on this edge is increased. The upper surface state splits off from bulk band for $\tilde{h}_2 < 0.37$ and the lower one splits off for $\tilde{h}_2 < -0.89$. The larger the coupling becomes the farther the surface state from bulk is located. Reducing the coupling between the first and second atom narrows the LDOS of the first atom. In the decoupling case ($\tilde{h}_2 = 1$, $\gamma' = 0$) the LDOS is a single atomic level at the reduced energy given by $\tilde{h}_1 = 0.8$ inside the bulk band range and no surface state is present. In the case of center of gravity shifts larger than the total bandwidth the atomic level of the first atom lies outside the bulk band of the chain. Consequently we have for each coupling between first and second atom at least one surface state. Such situation ($\tilde{h}_1 = 1.2$) is given in Figure 7. The atomic level at $\tilde{h}_1$ plays the role of a surface

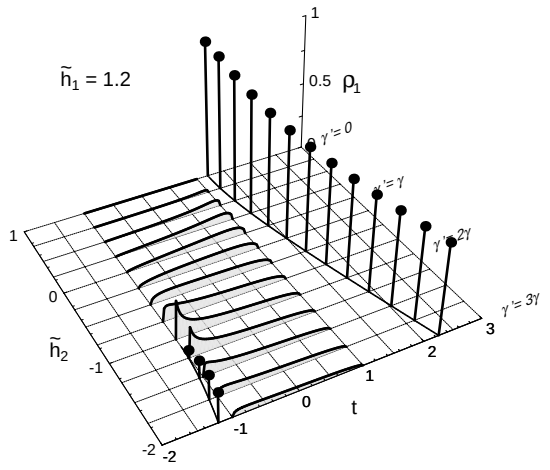

Fig. 7. LDOS of the first atom dependent of the reduced energy and the coupling between the first and second atom for a center of gravity shift is 1.2 total bandwidths.

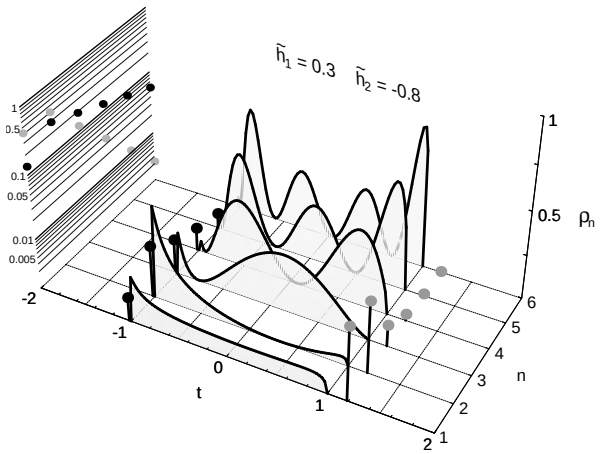

Fig. 8. Layer dependent LDOS for $n = 1, \ldots, 6$ in case of slightly shifted center of gravity of the first atom and increased hopping between first and second atom. The inset is a logarithmic plot of the spectral weights of surface states.

state. Within the bulk band range the LDOS vanishes. If the coupling is strong enough ($\tilde{h}_2 < -1.10$) an additional lower surface state occurs.

Now we are interested in the propagation of the surface states into the bulk. Figure 8 shows LDOS for the first six layers. The lower surface states are visualized by black points the upper ones by grey points. The spectral weight is given by the height in the 3-dimensional plot. Some general features (number of oscillations and zeros) presented in Figure 3 can be found again. The position in reduced energy of each surface state is fixed only the weight varies from layer to layer. For these parameters the maximum of the surface state weight is at the second atom not at the first. Starting from the second atom the weight of both surface state drops exponentially to zero in agreement to our expectations. This can easily be seen in the logarithmic plot in the inset. The lower surface state which is closer to the bulk band drops down slower than the upper one which is more far from bulk band. Now we have an complete picture of our chain model.

4 Application to the s.c. (100) surface of a semi-infinite crystal

In this section we investigate the surface states of a semi-infinite s.c. (100) crystal in detail.

4.1 Modification of Hopping

The Hamiltonian of the semi-infinite extended s.c. (100) crystal has the form (6)

$$\mathbf{H} = \sum_{\alpha\beta\mathbf{k}} T_{\alpha\beta}(\mathbf{k}) = \sum_{\mathbf{k}} \mathbf{h}(\mathbf{k}), \tag{45}$$

where $T_{\alpha\beta}(\mathbf{k})$ are the elements of the Bloch matrix and $\alpha, \beta = 1, 2, \ldots$ are layer indices. If the Bloch matrix for each wave vector $\mathbf{k}$ is of the form (15) (tridiagonal) then our method derived in Section 3 can be applied and can be interpreted as an ensemble of semi-infinite linear chains for each $\mathbf{k}$-point.

The presence of the surface manifests itself in a modification of hopping at least within the surface layer and the surface nearest layer. These modifications can be induced for example by reconstruction or by correlation effects [17]. This can be included in the mapping onto the semi-infinite linear chain $(\alpha(\mathbf{k}), \alpha'(\mathbf{k}), \gamma(\mathbf{k}), \gamma'(\mathbf{k}))$.

We investigate the surface in the tight binding approximation. In our special case the elements of the Bloch matrix are real. The site indices in the directions parallel to the surface are labeled by a Latin letter and the index counting the layer parallel to the surface is labeled by a Greek letter. The tight binding approximation can be written as

$$T_{ij}^{\alpha\beta} = \delta_{i,j\pm\Delta}^{\alpha\beta} T^{\alpha\alpha} + \delta_{ij}^{\alpha,\beta\pm1} T^{\alpha\beta} \tag{46}$$

where $\Delta = (0,1), (0,\bar{1}), (1,0), (\bar{1},0)$. $T^{\alpha\beta}$ is the hopping between the layers α and $\beta = \alpha \pm 1$ and $T^{\alpha\alpha}$ within the layer α. We describe these influences by change of the hopping within the first layer $T^{11} = \epsilon_{\|} T$ and the change of the hopping between the first and second layer by $T^{12} = \epsilon_{\perp} T$. This variation of hopping within the surface layer and between the surface layer and the surface nearest layer was part of numerical calculations performed on a local moment film in our previous paper [1]. We use the dispersions defined by equations (4, 5) and given in Appendix A,

$$\gamma_{\|}(\mathbf{k}) = 2\left(\cos(k_x a) + \cos(k_y a)\right), \tag{47}$$

$$\gamma_{\perp}(\mathbf{k}) = 1. \tag{48}$$

Thus the diagonal elements of the Hamiltonian and of the Bloch matrix are given by

$$h_{\mathbf{k}}^{11} = T_{\mathbf{k}}^{11} = \epsilon_{\|} T \gamma_{\|}(\mathbf{k}), \quad h_{\mathbf{k}}^{\alpha\alpha} = T_{\mathbf{k}}^{\alpha\alpha} = T\gamma_{\|}(\mathbf{k}), \tag{49}$$

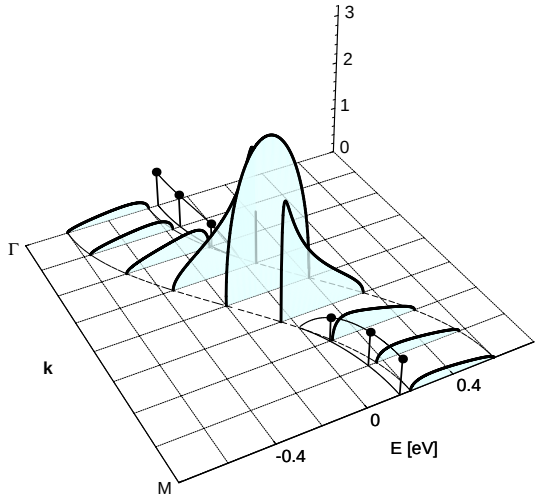

Fig. 9. Spectral density of surface layer with $\epsilon_\perp = 1$, $\epsilon_\parallel = 0.5$ as a function of the wave vector $\mathbf{k}$ for the $\overline{\Gamma}\overline{\mathrm{M}}$ direction.

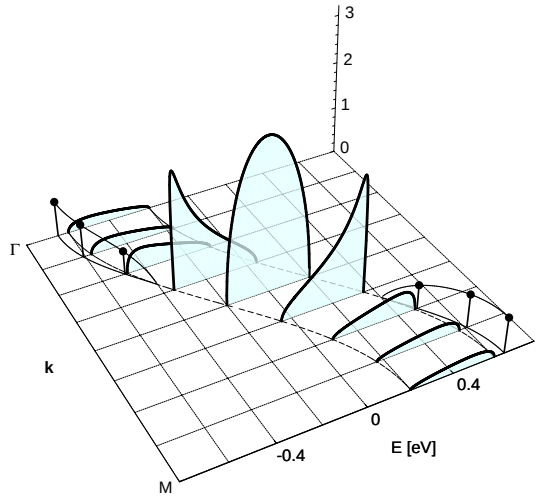

Fig. 10. The same as in Figure 9 but for $\epsilon_\perp = 1$, $\epsilon_\parallel = 1.5$.

and the first upper and lower diagonal elements by

$$h^{12}_{\mathbf{k}} = h^{21}_{\mathbf{k}} = T^{12}_{\mathbf{k}} = T^{21}_{\mathbf{k}} = \epsilon_\perp T\gamma_\perp(\mathbf{k}), \tag{50}$$
$$h^{\alpha+1,\alpha}_{\mathbf{k}} = h^{\alpha,\alpha+1}_{\mathbf{k}} = T^{\alpha+1,\alpha}_{\mathbf{k}} = T^{\alpha,\alpha+1}_{\mathbf{k}} = T\gamma_\perp(\mathbf{k}).$$

In case of the infinite s.c. (100) surface the parameters $\alpha(\mathbf{k})$, $\alpha'(\mathbf{k})$, $\gamma(\mathbf{k})$, and $\gamma'(\mathbf{k})$ are k-dependent *via* the dispersion equations (47, 48),

$$\alpha'(\mathbf{k}) = \epsilon_\parallel T\gamma_\parallel(\mathbf{k}), \tag{51}$$
$$\alpha(\mathbf{k}) = T\gamma_\parallel(\mathbf{k}),$$

$$\gamma'(\mathbf{k}) = -\epsilon_\perp T\gamma_\perp(\mathbf{k}), \tag{52}$$
$$\gamma(\mathbf{k}) = -T\gamma_\perp(\mathbf{k}).$$

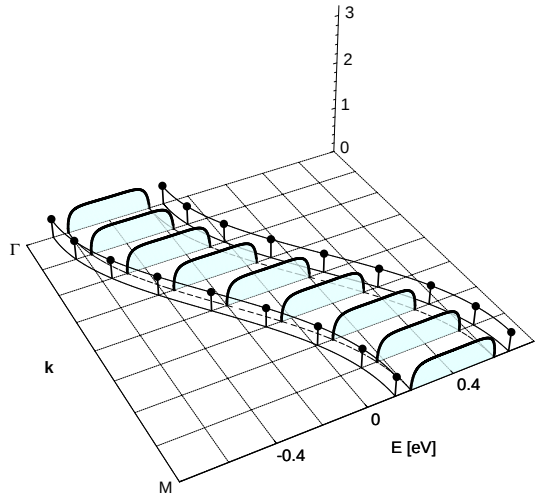

Fig. 11. The same as in Figure 9 but for $\epsilon_\parallel = 1$, $\epsilon_\perp = 2.5$.

4.2 Spectral density

We choose $T = -0.1$ eV in order to compare with our results in reference [1]. The next four Figures 9-12 show the spectral density of the surface layer for wave vectors of first Brillouin zone from $\overline{\Gamma}$ to $\overline{\mathrm{M}}$. The surface states are represented by a black line with a point on the top. Its height gives the spectral weight. The spectral density for each wave vector is normalized to one. The solid line connecting the surface states gives the $\mathbf{k}$-dependent spectral weight. The dashed lines limit the range of bulk bands in the two dimensional Brillouin zone.

First Figure 9 we let the hopping between the first and second layer unchanged ($\epsilon_\perp \equiv 1$). If we reduce the hopping within the surface layer to 50% one surface state splits off from the inner band edges starting from the $\overline{\Gamma}$ and $\overline{\mathrm{M}}$ point respectively. Around the center between $\overline{\Gamma}$ and $\overline{\mathrm{M}}$ no surface state can be found. The behavior at the $\overline{\mathrm{M}}$-point coincides with Figure 4 in our previous work [1]. The layer dependence of the spectral density for each wave vector $\mathbf{k}$ can be obtained by a plot like Figure 8 starting from the matching parameters (Eqs. (51, 52)) for the atomic chain. Regarding the $\mathbf{k}$ dependent spectral density we expect the corresponding local density of states (LDOS) of the first layer to be narrowed in this case because spectral weight is transfered to the inner side of dispersion curve.

Figure 10 represents the situation for inter layer hopping increased by 50%. The surface state is now on the outer side of the band. A broadening in the (LDOS) can be expected.

If we leave the hopping within the surface layer constant ($\epsilon_\parallel = 1$) and modify the hopping between the surface nearest layer by the factor $\epsilon_\perp = 2.5$ we get Figure 11. Because of equation (48) there is no variation only a shift of the center of gravity of spectral density. The shape at the $\overline{\mathrm{M}}$-point the same as Figure 5 in reference [1].

If we vary both the hopping within the surface layer by $\epsilon_\parallel = 1.5$ and the hopping between it and the surface nearest layer by $\epsilon_\perp = 2.0$ we get a situation plotted in Figure 12. Here exists for $\mathbf{k}$ nearby $\overline{\Gamma}$ or $\overline{\mathrm{M}}$ one surface state with large spectral weight at the outer side of the band and there are two surface states in the $\mathbf{k}$-region from $(0.3, 0.3)$ to $(0.6, 0.6)$.

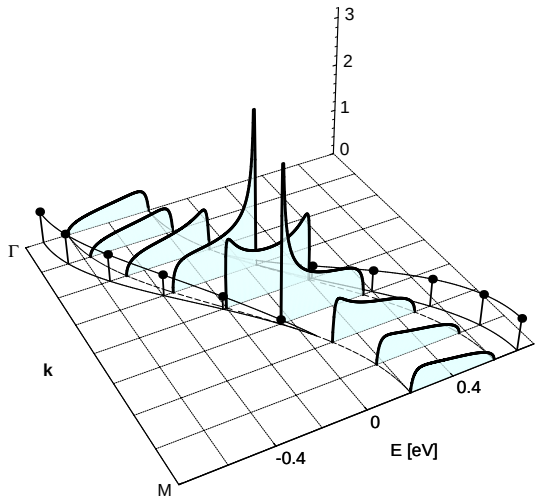

Fig. 12. The same as in Figure 9 but for $\epsilon_{\|} = 1.5$, $\epsilon_{\perp} = 1.8$.

Figure 13 shows for three values of hopping between the surface and surface nearest layer the spectral weight of the surface states as function of the wave vector of the two dimensional Brillouin zone between $\overline{\Gamma}$ and $\overline{\mathrm{M}}$ and as a function of the modification of hopping within the surface layer $\epsilon_{\|}$. The situation for any given pair of $\epsilon_{\|}$ and $\epsilon_{\perp}$ is given by the cut parallel to the **k**-axis.

In the first graph the hopping between the layers remains unchanged ($\epsilon_{\perp} = 1$). The cut for $\epsilon_{\|} \in (\frac{3}{4}, \frac{5}{4})$ has no intersections with the four dark or light gray shaded faces no surface states can occur. For larger modifications of hopping within the surface layer the regions in the 2-dimensional Brillouin where surface states exist become larger and the surface states are more pronounced. For $\epsilon_{\|} < \frac{3}{4}$ we have near the $\overline{\Gamma}$ point surface states above the bulk band (dark gray shaded face) and we have near the $\overline{\mathrm{M}}$ point of the two dimensional Brillouin zone surface states below the band (light gray shaded face). This is the situation plotted in Figure 9. For $\epsilon_{\|} > \frac{5}{4}$ we observe an analogous behavior except that the surface states near the $\overline{\Gamma}$ point are lower in energy than the band and those near the $\overline{\mathrm{M}}$ point are higher in energy with respect to the band. (Compare with Fig. 10.)

In the second graph $\epsilon_{\perp} = 1.41$ is chosen just before the limiting value of $\epsilon_{\perp} = \sqrt{2}$ which corresponds to $\tilde{h}_2 = 1 - \sqrt{2}$ for the linear chain. The four faces representing surface states below and above the bulk band are extended. For the limiting value $\epsilon_{\perp} = \sqrt{2}$ the four faces merge and on each point in the **k**, $\epsilon_{\|}$ parameter space exact one surface state exists except the lines $\epsilon_{\perp} \equiv 1$ and $\mathbf{k} \equiv (\frac{\pi}{2a}, \frac{\pi}{2a})$ where the spectral weight vanishes. For larger values of $\epsilon_{\perp}$ at least one surface state exists at each **k** point of the 2-dimensional Brillouin zone. The conditions for the existence of surface states apply to the spectra in our previous work [1].

The last graph $\epsilon_{\perp} = 1.8$ presents the plot for stronger modification of the hopping between the first and the second layer than the limit value $\epsilon_{\perp} > \sqrt{2}$. In this case the four faces cross each other. For values of $0.7 \lesssim \epsilon_{\|} \lesssim 1.3$ there are two intersections at the whole Brillouin therefore

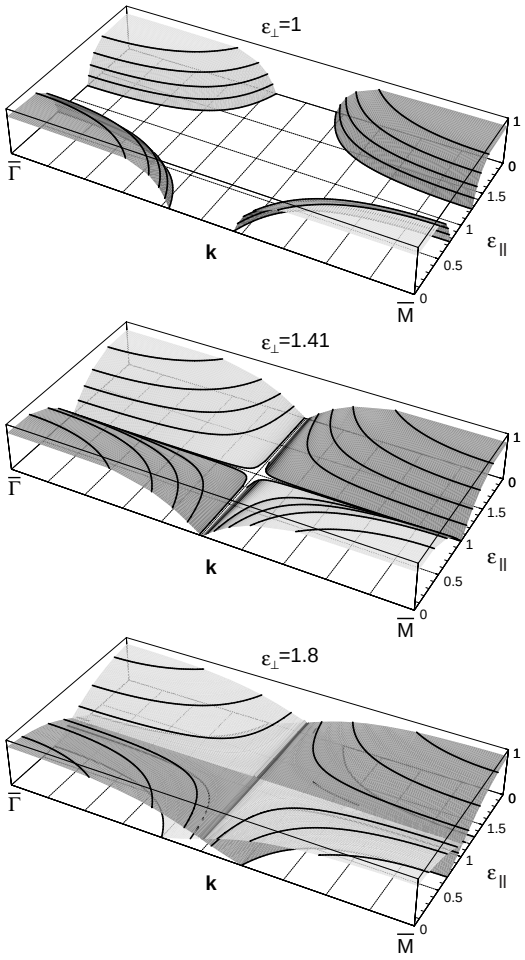

Fig. 13. Spectral weight of surface states at the surface layer for three values of the modified hopping between the first and second layer $\epsilon_{\perp} = 1, 1.41, 1.8$ dependent on the 2-dimensional wave vector $\mathbf{k} \in (\overline{\Gamma}, \overline{\mathrm{M}})$ and the modification of hopping within the surface layer $\epsilon_{\|} \in (0, 2)$. The dark gray shaded faces show surface states with an energy above the band and the light gray shaded ones show surface states below the band. The solid lines join points with equal spectral weight of surface state. They are spaced with 0.2 with respect to the spectral weight.

exist two surface states per **k** point at the whole Brillouin zone and for larger changes of $\epsilon_{\|} \lesssim 0.7$ or $\epsilon_{\|} \gtrsim 1.3$ only one surface state occur near the $\overline{\Gamma}$ or near the $\overline{\mathrm{M}}$ point and two surface states exists fore each **k** in between (*e.g.* Fig. 12).

5 Influence of spin exchange correlation

Now we include spin exchange correlation in our model. We investigate the surface states in a correlated s.c. (100) local-moment film as presented in reference [1]. We restudy the special case of a single electron in an empty conduction band and zero temperature which can be solved exactly in the framework of the $s-f$ model

(or ferromagnetic Kondo model). The Hamiltonian which can be written as:

$$\mathbf{H} = \sum_{ij\alpha\beta} \left(T_{ij}^{\alpha\beta} - \mu\delta_{ij}^{\alpha\beta} \right) c_{i\alpha\sigma}^{+} c_{j\beta\sigma} - J \sum_{i\alpha} \mathbf{S}_{i\alpha} \boldsymbol{\sigma}_{i\alpha} \quad (53)$$

describes with the first part the itinerant conduction electrons ($T_{ij}^{\alpha\beta}$ are the elements of the hopping matrix, μ is the chemical potential) and describes with the second part the interaction of the electrons and localized spins represented by $\mathbf{S}_{i\alpha}$. It is assumed that the system of the localized spins is completely ferromagnetic aligned at zero temperature. $c_{i\alpha\sigma}^{+}$ and $c_{j\beta\sigma}$ are, respectively, the creation and annihilation operators of an electron with spin σ ($\sigma = \uparrow, \downarrow$). J is the $s-f$ exchange constant and $\boldsymbol{\sigma}_{i\alpha}$ is the Pauli spin operator of the s-band electrons. The solution for the Green function of the local moment film is given by

$$\mathbf{G}_{\mathbf{k},\sigma} = \hbar \mathbf{D}_{\mathbf{k},\sigma}^{-1}, \quad (54)$$

where

$$(D_{\mathbf{k},\sigma})^{\alpha\beta} = -T_{\mathbf{k}}^{\alpha\beta} + \delta^{\alpha\beta}(E + \frac{1}{2} z_\sigma J\hbar S - \delta_{\downarrow\sigma} C_\alpha), \quad (55)$$

and $z_\uparrow = 1$, $z_\downarrow = -1$ correspond to the direction of the spin of the conduction band electron and characterize the direction of the shift of the spectrum dependent on the $s-f$ exchange coupling constant J. The layer dependent term C_α only occurs in the spin-$\downarrow$ spectrum.

Spin-↑-spectrum

In case of the spin-↑-electron the correlation switched on by J only shifts the spectrum rigidly by the constant energy $\Delta E = -\frac{1}{2} J\hbar S$ towards lower energies because the electron can not exchange its spin with the at zero temperature perfectly aligned local moment system. Consequently our analytical model presented in 4.1 and 4.2 is the exact solution for this case if we substitute α, α' by $\alpha, \alpha' + \Delta E$.

Spin-↓-spectrum

The term

$$C_\alpha = \frac{\frac{1}{2} J^2 \hbar^2 S B_\alpha}{1 - \frac{1}{2} J\hbar B_\alpha} \quad (56)$$

where

$$B_\alpha = \frac{1}{N} \sum_{\mathbf{k}} (D_{\mathbf{k}\uparrow})^{\alpha\alpha} \quad (57)$$

is a consequence of the possibility for a spin-$\downarrow$ electron to exchange its spin with the local moment system. For small values of the exchange coupling J a deformation of the free spin-$\downarrow$ spectral density results and the quasiparticle gets a finite lifetime. For stronger J the spectrum splits into two parts belonging to two different mechanisms of the spin exchange between the excited spin-$\downarrow$ electron and the system of the localized spins. One of these excitations can be commented on as the polarization of the direct spin surroundings of the electron due to a repeated emission and reabsorption of magnons. This results in a polaron-like quasiparticle which we call in the following the "magnetic polaron". The magnetic polaron is located at higher energies of the spectrum. The second possible excitation is the emission of a magnon by the original spin-$\downarrow$ electron without reabsorption, but necessarily with a spin flip of the electron. The result is a broad low-energy "scattering part" in the spectral density. The spin-flip process is only possible if there are spin-↑ states within reach. If we neglect the tiny magnon energies the scattering part occupies exactly the same energy range as the spin-↑ quasiparticle density of states. For details of the discussion see [1,18]. For qualitative understanding of surface states in the local moment film it is sufficient to assume the spin exchange correlation expressed by $C_\alpha(E)$ to be layer independent. This is reasonable because the values for J are small and the $B_\alpha(E)$ entering into is obtained by summation over the two dimensional Brillouin zone of the spin-↑-electron Green function. The small changes in the shape of those quantities within the layers closest to the surface are omitted. That means the effect of a narrowing for $\epsilon_\parallel < 1$ and of the broadening for $\epsilon_\parallel > 1$ ($\epsilon_\perp \equiv 1$) with respect to the situation in the bulk which drops down exponentially from the surface to the bulk is not present. The calculation presented here are performed using $C_\alpha = C_\infty$. Using the formula (5.52) in [19] we get

$$B_\infty(E) = \frac{1}{2\pi^2 |T|} \int_0^\pi \mathrm{d}\phi \; t \; \mathbb{K}(t) \quad (58)$$

where $t = 4|T|/(E - \Delta E - 2|T|\cos\phi)$ and $\mathbb{K}$ is the complete elliptic integral of the first kind. It is also possible to extend it to $C_1 \neq C_{\alpha>1} = C_\infty$ without any change in our chain model to include in a first step the layer dependence of the scattering part in the spectra. Figure 14 shows the results of this calculation. Fore the comparison the results of the numerical calculation for a thick local moment film from [1] (density plot Fig. 9) are presented in Figure 15. The local spin-$\downarrow$ density for the first, the second and a bulk layer is plotted for the $s-f$ exchange coupling $J = 0.3$. In the spectra of the first and second layer we observe near the $\overline{\Gamma}$ point and near the $\overline{\mathrm{M}}$ point of the 2-dimensional Brillouin zone the splitting off of a surface state from bulk band (layer ∞). The features observed for the case without correlation ($J = 0$) are rendered in the shape of the "magnetic polaron" part of the spectrum. For reduction of the hopping within the surface layer by $\epsilon_\parallel = 0.4 < 1$ the split off happens at the inner dispersion band side (compare Fig. 9) and for enhanced hopping $\epsilon_\parallel = 1.6 > 1$ the split off occurs on the outer side (compare Fig. 10). As a consequence the local density of states of the polaron band is narrowed for $\epsilon_\parallel < 1$ and broadened for $\epsilon_\parallel > 1$. The nearer to the band in energy the more pronounced is the scattering part. The largest scattering part is observable

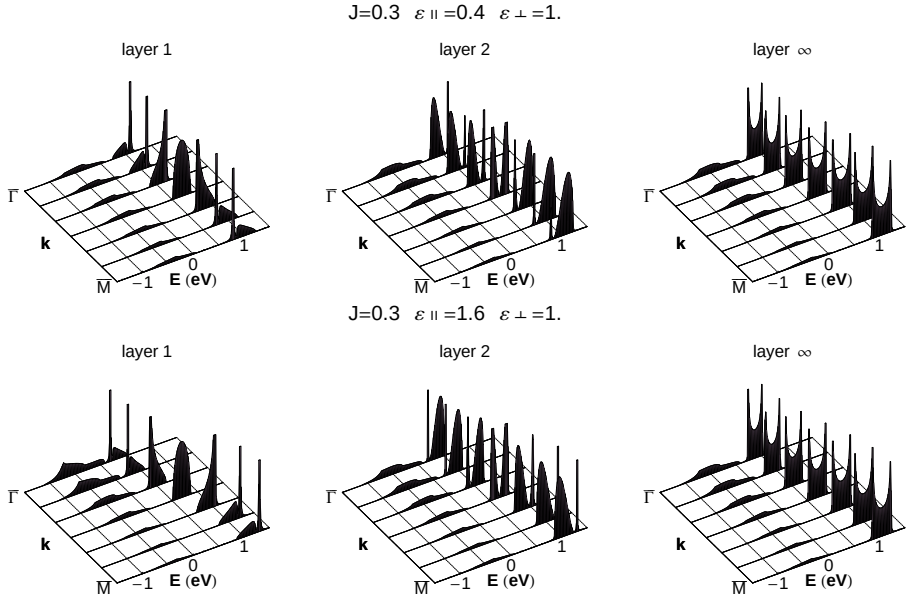

Fig. 14. Local spin-↓ spectral density of the first two layers and the bulk layer for the sf-exchange coupling constant $J = 0.3$ and modified hopping within the first layer ($\epsilon_{\|} = 0.4, 1.6$). The hopping between the layers remains constant.

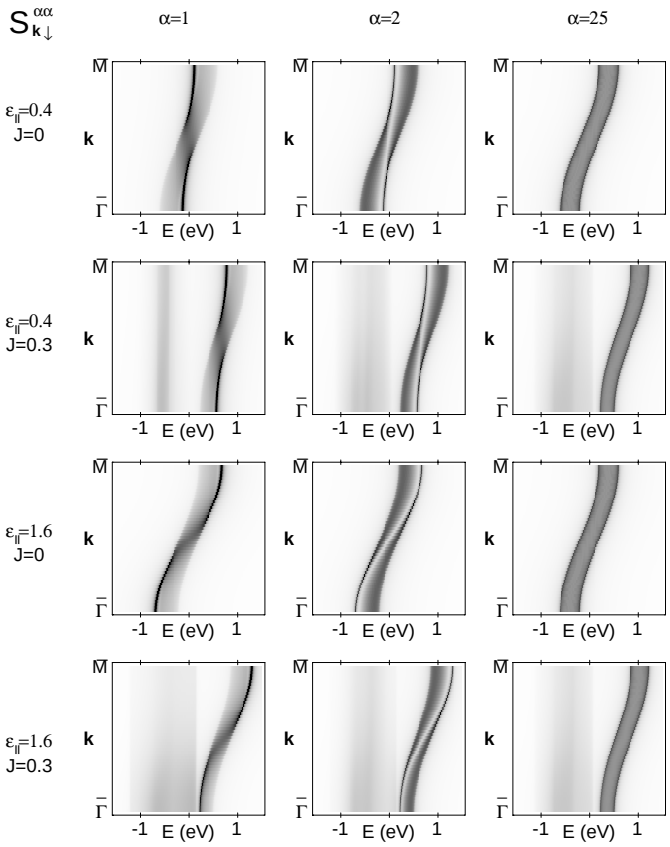

Fig. 15. Density plots of the (numerically calculated [1]) local spin-↓ spectral density of the $\alpha = 1, 2, 25$ layer of a 50 layer film as a function of energy and $\mathbf{k} \in (\overline{\Gamma}, \overline{\mathrm{M}})$ for two $s-f$ exchange coupling constants $J = 0, 0.3$ and modified hopping within the first layer ($\epsilon_{\|} = 0.4, 1.6$). The hopping between all layers remains constant.

in the spectrum of the surface layer at the $\overline{\Gamma}$ point in case of a surface state below the band ($\epsilon_{\|} = 1.6$). The shape of spectra and the mentioned features are identical with the numerical results for a 50 layer local moment film given in the density plot of Figure 15. The replacement of the layer dependent term C_α by its bulk expression has no visible consequences but in principle the scattering part should be a little bit narrowed for $\epsilon_{\|} < 1$ and a little bit broadened for $\epsilon_{\|} > 1$.

6 Conclusions

We have investigated the Green function of the semi-infinite linear chain in tight binding approximation. The problem of modification of the center of gravity of the band from the first atom and the coupling between the first and second atom is solved analytically exactly. One surface state occurs for center of gravity shifts larger than half bandwidth and two surface states are present if the coupling between first and second atom is enhanced by a factor larger than $\sqrt{2}$. A phase diagram is constructed. The spectral weight of surface states is evaluated analytically and drops down exponentially with distance from the surface to the bulk.

The obtained model is applicable to all surfaces which allow the k-dependent mapping which is possible within the tight binding approximation.

This kind of mapping is done for the s.c. (100) surface. The conditions for the existence of surface states mentioned in reference [1] have been proved. For sufficiently modified hopping within the surface layer by more than 25% one surface state splits off from bulk band. The existence of surface states for a given change of the hopping within the surface layer is dependent on the wave vector

of the two dimensional Brillouin zone and starts at the $\overline{\Gamma}$ and the $\overline{\mathrm{M}}$ point. If the hopping between surface layer and the surface nearest layer is enhanced by more than $\sqrt{2}$ two surface states show up, one below and one above the bulk band.

We included correlation in a simplified manner *e.g.* we assumed a layer independent self energy which has to be added to each diagonal element of the Hamiltonian of our chain model. In principle it is possible to introduce for the first layer a different self energy, too. But it is not necessary for getting a beautiful agreement with the results of the numerical evaluation for thick films [1]. The general structure of the spin-↑ spectrum is enriched by correlation (scattering part) also visible in the spin-↓ spectrum in the polaron part. In our calculations the energy range occupied by the scattering part of the spectrum is constant. For the exact result (using layer dependent self energy) one should expect a broadening of this range if a spin-↑ surface state splits off on the outer side of the dispersion curve. In this case there are surface states not only in the "magnetic polaron" part (δ-peak) but also in the scattering part (continuous).

This approach helps to basically understand the conditions for the appearance and the behavior of surface states and will be completed by studies on *the temperature dependent behavior of surface states on ferromagnetic semiconductors* [2].

This work was supported by the Deutsche Forschungsgemeinschaft within the Sonderforschungsbereich 290 ("Metallische dünne Filme: Struktur, Magnetismus, und elektronische Eigenschaften"). One of us (R.S.) gratefully acknowledges the support by the Studienstiftung des deutschen Volkes.

Appendix A: Dispersion for different surface geometries

The dispersion is calculated using equations (4, 5).

s.c. (100)

$$\begin{aligned}\gamma_{\parallel}(\mathbf{k}) &= 2\left(\cos(k_x a) + \cos(k_y a)\right)\\ \gamma_{\perp}(\mathbf{k}) &= 1\end{aligned} \tag{A.1}$$

s.c. (110)

$$\begin{aligned}\gamma_{\parallel}(\mathbf{k}) &= 2\cos(k_x a)\\ \gamma_{\perp}(\mathbf{k}) &= 2\cos(\sqrt{2}k_y a)\end{aligned} \tag{A.2}$$

s.c. (111)

$$\begin{aligned}\gamma_{\parallel}(\mathbf{k}) &= 0\\ \gamma_{\perp}^{-}(\mathbf{k}) &= \mathrm{e}^{\mathrm{i}\sqrt{\frac{2}{3}}k_x a} + \mathrm{e}^{-\mathrm{i}\sqrt{\frac{1}{6}}k_x a}\cdot 2\cos\left(\frac{\sqrt{2}}{2}k_y a\right)\end{aligned} \tag{A.3}$$

b.c.c. (100)

$$\begin{aligned}\gamma_{\parallel}(\mathbf{k}) &= 0\\ \gamma_{\perp}(\mathbf{k}) &= 2\cos[(k_x+k_y)\frac{a}{2}] + 2\cos[(k_x-k_y)\frac{a}{2}]\end{aligned} \tag{A.4}$$

b.c.c. (110)

$$\begin{aligned}\gamma_{\parallel}(\mathbf{k}) &= 2\cos(k_x\tfrac{a}{2} + k_y\tfrac{a}{\sqrt{2}}) + 2\cos(k_x\tfrac{a}{2} - k_y\tfrac{a}{\sqrt{2}})\\ \gamma_{\perp}(\mathbf{k}) &= 2\cos(k_x\frac{a}{2})\end{aligned} \tag{A.5}$$

f.c.c. (100)

$$\begin{aligned}\gamma_{\parallel}(\mathbf{k}) &= 2[\cos((k_x+k_y)\frac{a}{2}) + \cos((k_x-k_y)\frac{a}{2})]\\ \gamma_{\perp}(\mathbf{k}) &= 2(\cos[k_x\frac{a}{2}] + \cos[k_y\frac{a}{2}])\end{aligned} \tag{A.6}$$

f.c.c. (111)

$$\begin{aligned}\gamma_{\parallel}(\mathbf{k}) &= 2[\cos(\sqrt{\tfrac{3}{8}}k_x + \sqrt{\tfrac{1}{8}}k_y)a) + \cos(\sqrt{\tfrac{3}{8}}k_x - \sqrt{\tfrac{1}{8}}k_y)a)\\ &\quad + \cos(\sqrt{\tfrac{1}{2}}k_y a)]\\ \gamma_{\perp}^{-}(\mathbf{k}) &= \mathrm{e}^{\mathrm{i}\sqrt{\frac{1}{6}}k_x a} + \mathrm{e}^{-\mathrm{i}\sqrt{\frac{1}{24}}k_x a}2\cos\left(\frac{\sqrt{2}}{4}k_y a\right)\end{aligned} \tag{A.7}$$

Appendix B: Analytical representation of Green function

Using equation (8) the Green function is given by

$$\mathbf{G}^0(E) = -\frac{\hbar}{\gamma}\begin{pmatrix} -2t & -1 & 0\cdots\\ -1 & -2t & -1 & \ddots\\ 0 & -1 & -2t & \ddots\\ \vdots & \ddots & \ddots & \ddots\end{pmatrix}^{-1}. \tag{B.1}$$

Equation (B.1) reads

$$\mathbf{G}^0(E) = -\frac{\hbar}{\gamma}\,\mathbf{M}^{-1} \tag{B.2}$$

where $\mathbf{M}$ is given by

$$\mathbf{M} = \begin{pmatrix} 2\cos\theta & -1 & 0\cdots\\ -1 & 2\cos\theta & -1 & \ddots\\ 0 & -1 & 2\cos\theta & \ddots\\ \vdots & \ddots & \ddots & \ddots\end{pmatrix}. \tag{B.3}$$

The analytic solution of the inverse matrix $\mathbf{M}^{-1}$

$$\left(\mathbf{M}^{-1}\right)_{kl} = m_{kl} = \left(\mathrm{e}^{\mathrm{i}(k+l)\theta} - \mathrm{e}^{\mathrm{i}|k-l|\theta}\right) \Big/ (2\mathrm{i}\sin\theta) \tag{B.4}$$

is given by Wax [20].

Appendix C: Inversion of matrix A

The matrix inversion is achieved by the simple rule

$$\left(\mathbf{A}^{-1}\right)_{ij} = \frac{\det \mathbf{A}_{ji}}{\det \mathbf{A}}, \tag{C.1}$$

where $\mathbf{A}_{ji}$ is the adjunct matrix to $\mathbf{A}$ obtained by deleting the j-th row and i-th column. The inverse matrix is given by

$$\mathbf{A}^{-1} = \frac{1}{\det \mathbf{A}} \begin{pmatrix} a_{22} & -a_{12} & 0 & \cdots \\ -a_{21} & a_{11} & 0 & \cdots \\ \begin{vmatrix} a_{21} & a_{31} \\ a_{22} & a_{32} \end{vmatrix} & -\begin{vmatrix} a_{11} & a_{31} \\ a_{12} & a_{32} \end{vmatrix} & \det \mathbf{A} & \ddots \\ \begin{vmatrix} a_{21} & a_{41} \\ a_{22} & a_{42} \end{vmatrix} & -\begin{vmatrix} a_{11} & a_{41} \\ a_{12} & a_{42} \end{vmatrix} & 0 & \ddots \\ \vdots & \vdots & \vdots & \ddots \end{pmatrix}, \tag{C.2}$$

where $a_{ij} = (\mathbf{A})_{ij}$ and

$$\det \mathbf{A} = \lambda = \begin{vmatrix} a_{11} & a_{21} \\ a_{12} & a_{22} \end{vmatrix}. \tag{C.3}$$

Appendix D: Calculation of spectral weights

The inverse of equation (29) for $z \in \mathbb{R}$ is given by

$$\left.\begin{array}{ll} z < -1 & z(t) = -t - \sqrt{t^2 - 1} \\ -1 \le z < 0 & z(t) = -t + \sqrt{t^2 - 1} \\ 0 \le z < 1 & z(t) = -t - \sqrt{t^2 - 1} \\ z > 1 & z(t) = -t + \sqrt{t^2 - 1} \end{array}\right\} \begin{array}{l} t > 0, \\ \\ t < 0. \end{array} \tag{D.1}$$

The dependence $z(t)$ given in equation (D.1) is to use for evaluate the correct limit. We make the differentiation:

1. $\tilde{h}_2 = 0$
   If $|\tilde{h}_1| > \frac{1}{2}$, the only surface state is given by equation (36)

   $$z_{1(2)} = -2\tilde{h}_1. \tag{D.2}$$

   The denominator (31) simplifies to

   $$\lambda(z) = z^{-1}(z + 2\tilde{h}_1). \tag{D.3}$$

   (a) $\tilde{h}_1 < -\frac{1}{2}$, one surface state below bulk band ($z_1 > 1$, $t_1 < -1$)
   If we pay attention to equation (D.1) we have to use $z = -t + \sqrt{t^2 - 1}$ and $z_1 = -t_1 + \sqrt{t_1^1 - 1}$. The result is

   $$\alpha_1^{(1)} = -2\ \frac{\sqrt{t_1^2 - 1}}{t_1 - \sqrt{t_1^2 - 1}}\,. \tag{D.4}$$

   (b) $\tilde{h}_1 > \frac{1}{2}$, one surface state above bulk band ($z_2 < -1$, $t_2 > 1$)
   In an analogous way we obtain

   $$\alpha_2^{(1)} = -2\ \frac{\sqrt{t_2^2 - 1}}{-t_2 - \sqrt{t_2^2 - 1}}\,. \tag{D.5}$$

2. $\tilde{h}_2 < 0$
   There are two solutions of equation (31) ($z_1 > 0 > z_2$)
   λ can be written as

   $$\lambda(z) = z^{-2}\,(z - z_1)(z - z_2) \tag{D.6}$$

   (a) $|z_{1,2}| > 0$, two surface states one above one below bulk band

   $$\begin{aligned} \alpha_1^{(1)} &= \frac{2\sqrt{t_1^2 - 1}}{t_2 + \sqrt{t_2^2 - 1} - t_1 + \sqrt{t_1^2 - 1}} \\ \alpha_2^{(1)} &= \frac{2\sqrt{t_2^2 - 1}}{t_2 + \sqrt{t_2^2 - 1} - t_1 + \sqrt{t_1^2 - 1}} \end{aligned} \tag{D.7}$$

   (b) $0 < z_1 \le 1$ and $z_2 < -1$, one surface state above bulk band

   $$\alpha_2^{(1)} = \frac{2\sqrt{t_2^2 - 1}}{t_2 + \sqrt{t_2^2 - 1} - t_1 - \sqrt{t_1^2 - 1}} \tag{D.8}$$

   (c) $z_1 > 1$ and $-1 \le z_2 < 0$, one surface state below bulk band

   $$\alpha_1^{(1)} = \frac{2\sqrt{t_1^2 - 1}}{t_2 - \sqrt{t_2^2 - 1} - t_1 + \sqrt{t_1^2 - 1}}\,. \tag{D.9}$$

3. $1 \ge \tilde{h}_2 > 0$
   There are two solutions possible if the square root in equation (31) is positive. Both have the same sign. The larger in absolute value gives a surface state if $|\tilde{h}_1| > \frac{1}{2} + \tilde{h}_2 - \frac{1}{2}\tilde{h}_2^2$.
   (a) $z_2 < -1 < z_1 < 0$

   $$\alpha_2^{(1)} = \frac{2\sqrt{t_2^2 - 1}}{-t_1 + \sqrt{t_1^2 - 1} + t_2 + \sqrt{t_2^2 - 1}} \tag{D.10}$$

   (b) $0 < z_2 < 1 < z_1$

   $$\alpha_1^{(1)} = \frac{2\sqrt{t_1^2 - 1}}{-t_1 + \sqrt{t_1^2 - 1} + t_2 + \sqrt{t_2^2 - 1}}\,. \tag{D.11}$$

References

1. R. Schiller, W. Müller, W. Nolting, Eur. Phys. J. B **2**, 249 (1998).
2. R. Schiller, W. Müller, W. Nolting, J. Phys. Cond. Matter **11**, 9589 (1999).
3. I. Tamm, Phys. Z. Sowjet. **1**, 733 (1932).

4. R.H. Fowler, Proc. R. Soc. London, Ser. A **141**, 56 (1933).
5. A.A. Sokolov, Z. Phys. **89**, 806 (1934).
6. A.W. Maue, Z. Phys. **94**, 717 (1935).
7. E.T. Goodwin, Proc. R. Soc. London, Ser. A **35**, 205 (1939).
8. W. Shockley, Phys. Rev. **56**, 317 (1939).
9. S.G. Davison, J.D. Levine, Solid State Phys. **25**, 1 (1970).
10. S.G. Davison, M. Stręślicka, *Basic Theory of Surface States* (Clarendon press, Oxford, 1992).
11. R. Haydock, in *Solid State Physics*, edited by H. Ehrenreich, F. Seitz, D. Turnbull (Academic press, N.Y., 1980), Vol. 35, p. 237.
12. A.A. Maradudin, E.Q. Montoll, G.H.W.I.P. Ipatova, *Solid State Phys.* (Academic Press N.Y., New York, 1971), Suppl. 3.
13. J. Pollmann, *Festkörperprobleme XX* (Vieweg, Braunschweig, 1980).
14. P.L. Taylor, *A quantum approach to the solid state* (Prentice-Hall, Englewood Cliffs, 1970).
15. E.-N. Foo, M.F. Thorpe, Surf. Sci. **57**, 323 (1976).
16. D. Kalstein, P. Soven, Surf. Sci. **26**, 85 (1971).
17. M. Potthoff, W. Nolting, Phys. Rev. B **59**, 2549 (1999).
18. R. Schiller, W. Müller, W. Nolting, J. Magn. Magn. Mater. **169**, 39 (1997).
19. E.N. Economou, *Green's Functions in Quantum Physics*, Vol. 7 of *Solid-State Sciences* (Springer, Berlin, 1990), 2nd edn.
20. *Selected papers on noise and stochastic processes*, edited by N. Wax (Dover Publications, New York, 1954), p. 301.